Round Robin-Based Synchronization Control for Discrete-Time Complex Networks With Probabilistic Coupling Delay and Deception Attacks

Yan Li, Feiyu Song, Jinliang Liu,
Xiangpeng Xie, *Senior Member, IEEE*, Engang Tian, and Shumin Fei

***Abstract*—Synchronization control is an important issue in complex networks (CNs), but the specific realization is generally influenced by many factors. In this article, by taking into accounts of the coupling effect and cyber attacks, we dedicate to design an efficient synchronization control approach for discrete-time CNs. Given that the coupling among nodes in CNs inevitably introduces the internode data exchange, round robin (RR) protocol is adopted to prevent data collision caused by the limitation of communication resources. Moreover, a probabilistic interval model is employed to capture the characteristics of the coupling delay, i.e., the delay of the internode data transmission. The deception attacks launched on the multichannel-enabled communication network between controllers and actuators of nodes in CNs are also considered. Then, a synchronization error model is established to describe the concerned synchronization control problem. By defining appropriate Lyapunov–Krsasovskii function, the sufficient conditions for the stability of the envisioned synchronization error system are obtained, and the design method for controllers is proposed subsequently. Simulations are finally conducted to demonstrate the validity of the work.**

***Index Terms*—Complex networks (CNs), deception attacks, probabilistic interval coupling delay, round robin (RR) protocol.**

I. Introduction

NOWADAYS, with the soaring of the complexity and scale of real-world systems, complex networks (CNs) are considered as an attractive architecture to describe many practical systems, such as power grids, transportation systems, and social networks [1], [2]. Typically, CN is made up with lots of nodes based on the certain topology, and each node in the network represents an entity with dynamical behaviors. The widespread application of CNs, however, leads to many challenging issues, e.g., state estimation, filter design, synchronization control, and the latter is particularly important since that synchronization is a natural requirement in CNs [3], [4]. Many research efforts have been paid on synchronization control for CNs and lots of achievements have been gotten accordingly. To mention a few, the fixed-time synchronization problem of CNs with both coupling and internal delays was investigated in [5]; the exponential synchronization of CNs under periodically intermittent noise was studied in [6]; the partial synchronization and multiclustering synchronization for CNs were discussed in [7] and [8], respectively. In addition to the aforementioned studies focused on continuous-time CNs, great research attentions have been devoted in synchronization control of discrete-time CNs due to the increasing volume of digital signals transmitted in physical systems. For instance, the event-based synchronization issue for discrete-time nonlinear CNs with identical nodes and disturbance was studied in [9]; Li et al. [10] addressed the synchronization issue for discrete-time delayed CNs with limited communication bandwidth; under the scenario of packet dropouts, the synchronization control for dynamical CNs was discussed in [11]. In view of this, this article will focus on discrete-time CNs to explore the synchronization control approach.

In order to design practical synchronization method for CNs, some potential influence factors should be seriously concerned. Toward this end, the coupling relationship among nodes has attracted interests of scholars. The coupling will result in information exchange among interconnected nodes, and some researches were successfully conducted based on the assumption that each node can receive signals from all of the connected neighbors [12], [13]. Nevertheless, given the limited bandwidth resources, the simultaneous communication between one node and its adjacent peers can hardly be realized. For avoiding data collision, an efficient solution is to use communication protocols to appropriately arrange the transfer of data that with the same destination. Round robin (RR) protocol, as a simple and feasible communication protocol, has been widely recognized by the industry [14]. Following RR protocol, competitors will be scheduled periodically, and only one node will be authorized to access the desired

Manuscript received 14 December 2023; accepted 14 March 2024. Date of publication 9 April 2024; date of current version 18 June 2024. This work was supported by the National Natural Science Foundation of China under Grant 61973152, Grant 62022044, and Grant 62273174. This article was recommended by Associate Editor H. Zhang. *(Corresponding author: Jinliang Liu.)*

Yan Li and Feiyu Song are with the College of Information and Engineering, Nanjing University of Finance and Economics, Nanjing 210023, Jiangsu, China (e-mail: ylnjue@163.com; songfeiyu29@163.com).

Jinliang Liu is with the School of Computer Science, Nanjing University of Information Science and Technology, Nanjing 210044, Jiangsu, China (e-mail: liujinliang@vip.163.com).

Xiangpeng Xie is with the Institute of Advanced Technology, Nanjing University of Posts and Telecommunications, Nanjing 210023, Jiangsu, China (e-mail: xiexiangpeng1953@163.com).

Engang Tian is with the School of Optical-Electrical and Computer Engineering, University of Shanghai for Science and Technology, Shanghai 200093, China (e-mail: tianengang@163.com).

Shumin Fei is with the School of Automation, Southeast University, Nanjing 210096, Jiangsu, China (e-mail: smfei@seu.edu.cn).

Color versions of one or more figures in this article are available at https://doi.org/10.1109/TSMC.2024.3378773.

Digital Object Identifier 10.1109/TSMC.2024.3378773

communication channel at each moment. In literatures, some important results have been presented for CNs with RR protocol under diverse applications [15], [16], but few works have studied RR-based synchronization control over CNs, which greatly motivates our study.

Although RR protocol can be adopted to manage the data exchange among interconnected nodes in CNs, the coupling delay can still occur due to the poor quality of devices, the interference/noise of channels, and etc [17]. To fully investigate the influence of the coupling delay on the synchronization problem of CNs, abundant researches have been reported. In [18], taking a constant coupling delay into consideration, an event-triggered impulsive control strategy was designed for the exponential synchronization over CNs. Given the random occurrence and time-vary of delays in practice, the studies concerned on CNs with the probabilistic coupling delay are also presented. By using a Bernoulli parameter to describe whether the coupling delay occurred, the synchronization issue for CNs with Markovian jump was explored in [19]. Cheng et al. [20] discussed the synchronization for discrete-time CNs with the coupling delay valued in a finite value set based on a given probability distribution. Considering that the physical coupling delay may take some large (small) values with low (high) probability, synchronization problem for CNs affected by the probabilistic interval coupling delay has been raised, and has received considerable research attentions [21], [22]. In this article, while conducting the synchronization control issue over discrete-time CNs, we will take the probabilistic interval coupling delay into account, and simultaneously consider using RR protocol to schedule data exchanged among nodes. Such integrated concern on the introduced coupling effect, i.e., the data collision among relative nodes and the coupling delay, differs our work from the discussed related researches.

Actually, besides the influence induced by coupling, cyber attacks launched on the communication network employed for intranode signal transmission, are acknowledged as another critical factor which impacts the design of synchronization method for CNs [23], [24], [25]. In general, replay attacks [26], [27], denial-of-service (DoS) attacks [13], [28] and deception attacks [29], [30], [31], [32] are three types of cyber attacks that have been most extensively studied. Among which, deception attacks have strong destroying power and can hardly be detected since that attackers always tamper correct data with malicious data, and then obtain particular concerns. For example, focusing on deception attacks that modify system state information, the secure path tracking control and H_∞ output feedback control over networked control systems were investigated in [30] and [31], respectively. Furthermore, some of recent studies have concentrated on the scenario that adversaries falsify control signals, i.e., the deception attacks occur on the network between controllers and actuators (referred to as N-CA), which will result in more challenging security issues [32], [33]. We also would like to note that the network for CNs now tends to be divided into multiple channels for efficient bandwidth sharing. Nevertheless, the bandwidth-sliced network can easily encourage asynchronous deception attacks, i.e., each of communication channels is compromised by a different deception attack. Despite some research attentions have been paid on asynchronous deception attacks aimed at control signals [34], [35], [36], to the best of our knowledge, under deception attacks launched on the N-CA, the synchronization control for RR-based discrete-time CNs with probabilistic interval coupling delay has not been explored.

In light of the above investigation, this article endeavors to propose an effective synchronization control approach for discrete-time CNs by comprehensively studying the mentioned influence of coupling and deception attacks. The main contributions of the work can be enumerated as follows.

1) The synchronization issue for RR-enabled discrete-time CNs with probabilistic interval coupling delay and asynchronous deception attacks occurred on the N-CA, is studied for the first time.
2) A novel synchronization error system model is established, then the synchronization control for the envisioned discrete-time CN affected by multifactors is transformed to guarantee the stability of the constructed synchronization error system.
3) The sufficient conditions are derived to assure the asymptotic stability of the synchronization error system, and the synchronization controllers are devised accordingly.
4) The efficiency of the proposed synchronization method is properly evaluated by conducting simulations over CNs with complete graph and noncomplete graph topologies.

The remainder of this article is arranged as follows. In Section II, the system model is described and the problem formulation is presented. In Section III, some sufficient conditions are derived for the considered CN to ensure the desired synchronization, and the controllers gains are calculated accordingly. The performance of the proposed synchronization control method is evaluated by simulations in Section IV. The conclusion of this article is given in Section V.

II. System Model and Problem Formulation

The following discrete-time CN system with N nodes, i.e., $\text{node}_1, \text{node}_2, \ldots, \text{node}_N$, is considered:

$$\begin{aligned} x_i(k+1) = Ax_i(k) + Bf(x_i(k)) + \sum_{j=1}^{N} c_{ij}\Gamma_1 x_j(k) \\ + \sum_{j=1}^{N} c_{ij}\Gamma_2 x_j(k-\tau(k)) + Du_i(k) \end{aligned} \tag{1}$$

where $1 \leq i \leq N$; $x_i(k) \in \mathbb{R}^{n_x}$ and $u_i(k) \in \mathbb{R}^{n_u}$ represent the state information and control input of node_i, respectively; $f : \mathbb{R}^{n_x} \to \mathbb{R}^{n_x}$ is a given nonlinear function; $\tau(k)$ names the time-varying probabilistic coupling delay which will be described shortly; $C = [c_{ij}]_{N\times N}$ is the outer-coupling matrix that is used for denoting the coupling configuration of the CN, in which $c_{ij} \geq 0$ $(1 \leq i \neq j \leq N)$, $c_{ii} = -\sum_{j=1, j\neq i}^{N} c_{ij}$ $(1 \leq i \leq N)$, and $c_{ij} > 0$ means that there is a link from node_i to node_j; $\Gamma_1 = \text{diag}\{\mu_1^1, \mu_1^2, \ldots, \mu_1^{n_x}\}$ and $\Gamma_2 = \text{diag}\{\mu_2^1, \mu_2^2, \ldots, \mu_2^{n_x}\}$ are the inner-coupling matrices, where μ_b^d $(b = 1, 2;\ d = 1, 2, \ldots, n_x)$ represents the coupling strength and $\mu_b^d \neq 0$ further indicates that two coupled nodes are linked through the dth component of the corresponding state variable; it is obviously that the outer-coupling and inner-coupling matrices jointly depict the coupling relationship among nodes in the CN; and A, B, and D are constant matrices with real numbers and suitable dimensions.

Assumption 1 [37]: It is assumed that the function $f(\cdot)$ in (1) is a continuous and bounded nonlinear function, and satisfies the following condition for any m_1 and m_2:

$$\iota_o \leq \frac{f_o(m_1) - f_o(m_2)}{m_1 - m_2} \leq \nu_o, o = 1, 2, \ldots, n_x \tag{2}$$

where $f_o(\cdot)$ is the oth element of $f(\cdot)$, ι_o, and ν_o are known constants which can be zero, negative, or positive.

Given that the model of each node is the same in the considered CN, then the structure of node$_i$ ($1 \leq i \leq N$) is specifically shown in Fig. 1. As presented, node$_i$ is connected with λ_i neighbors ($1 \leq \lambda_i \leq N-1$), i.e., node$_{i^1}$, node$_{i^2}$, ..., node$_{i^{\lambda_i}}$ ($1 \leq i^j \neq i \leq N, 1 \leq j \leq \lambda_i$), where the λ_i neighbors are sorted according to the increasing subscript order of them, i.e., $i^1 < i^2 < \cdots < i^{\lambda_i}$, for easy description. An isolated node $s(k+1) = As(k) + Bf(s(k))$ is embedded with node$_i$, then the dynamic error between node$_i$ and the isolated node can be represented as $e_i(k) = x_i(k) - s(k)$. With the introducing of the isolated node and following the similar setting in [11], the signal transmitted from node$_i$ to its connected neighbors is updated as $e_i(k)$, and the signals received by node$_i$ from its connected neighbors are $e_{i^1}(k)$, $e_{i^2}(k)$,..., $e_{i^{\lambda_i}}(k)$. Furthermore, the N-CA is assumed to be divided into N channels and channel i is assigned for node$_i$, the channel is envisioned to be subjected to a deception attack denoted as DA_i.

On the basis of the above description about the node structure, a synchronization error system can be constructed as follows:

$$\begin{aligned} e_i(k+1) &= x_i(k+1) - s(k+1) \\ &= Ae_i(k) + Bg_i(k) + \sum_{j=1}^{N} c_{ij}\Gamma_1 e_j(k) \\ &\quad + \sum_{j=1}^{N} c_{ij}\Gamma_2 e_j(k-\tau(k)) + Du_i(k) \end{aligned} \tag{3}$$

where $g_i(k) = f(x_i(k)) - f(s(k))$. In the remainder of the section, we then update the established synchronization error model by taking RR protocol, probabilistic interval coupling delay and asynchronous deception attacks into consideration.

Remark 1: In this article, N isolated nodes with uniform model are deployed, each of which is embedded with a node in the considered CN as presented in Fig. 1. Then, the synchronization of the CN can be realized by synchronizing each node to its co-located isolated node in a decentralized manner.

A. RR Protocol

In the CN, each node will receive signals from all its connected neighbors. To prevent data conflict caused by limited network bandwidth, RR protocol is used for each node to arrange data transmission. Without loss of generality, we then focus on the operation of RR protocol implemented on node$_i$ ($1 \leq i \leq N$).

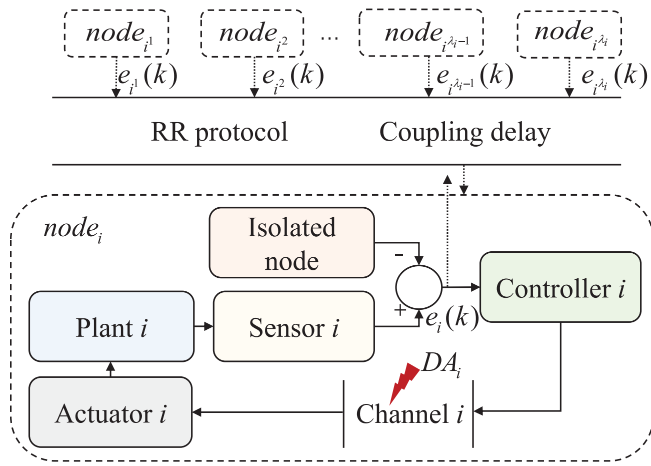

Fig. 1. Structure of node$_i$ in the considered CN.

Let $\Lambda_i = \{\text{node}_{i^1}, \text{node}_{i^2}, \ldots, \text{node}_{i^{\lambda_i}}\}$, then only one node in Λ_i is selected to send signals to node$_i$ at a time instant by following RR protocol. Specifically, the subscript of the selected neighboring node at time instant k ($k > 0$), denoted by $q_i(k)$, is defined as

$$q_i(k) = i^{p_i(k)} \tag{4}$$

where

$$p_i(k) = \text{mod}(k + p_i(0) - 1, \lambda_i) + 1.$$

mod refers to the modulus operator and $p_i(0)$ is a given initial value with $1 \leq p_i(0) \leq \lambda_i$.

Denoting $q(k) = \{q_1(k), q_2(k), \ldots, q_N(k)\}$, it is obviously that $q(k)$ is a periodic sequence with the cycle of Z time instants, where $Z = \text{LCM}(\lambda_1, \lambda_2, \ldots, \lambda_N)$, and LCM is an abbreviation for least common multiple. In other words, we have

$$q(k) = q(\text{mod}(k-1, Z) + 1). \tag{5}$$

Remark 2: In engineering practice, RR protocol has been widely used for many applications, such as CPU assignment in real-time systems, resource allocation in cloud computing, and task scheduling in multitasking systems. In this work, RR protocol is used for each node$_i$ ($1 \leq i \leq N$) to avoid data collision, and is specifically depicted by (4) and (5). Following (4), the λ_i neighbors of node$_i$ will be scheduled periodically, and only one neighbor can transmit signal to node$_i$ at each time instant. Then, the periodical feature of the data transmission of all nodes incurred by the RR protocol is appropriately reflected by (5). Actually, the mathematical formulation of RR protocol can be diverse as long as the characteristics of RR protocol are satisfied.

Under the depicted RR protocol, a binary variable $\omega_{ij,q_i(k)}$ ($1 \leq i \neq j \leq N$) is defined to denote whether or not node$_j$ can send signals to node$_i$ at time instant k, i.e., $\omega_{ij,q_i(k)} = 1$ if $j = q_i(k)$, otherwise $\omega_{ij,q_i(k)} = 0$ (we further set $\omega_{ii,q_i(k)} = 1$ for uniform description). Then, the synchronization error system model (3) can be rewritten as

$$e_i(k+1) = Ae_i(k) + Bg_i(k) + \sum_{j=1}^{N} \omega_{ij,q_i(k)} c_{ij} \Gamma_1 e_j(k) + \sum_{j=1}^{N} \omega_{ij,q_i(k)} c_{ij} \Gamma_2 e_j(k-\tau(k)) + Du_i(k). \quad (6)$$

B. Probabilistic Interval Coupling Delay

In the synchronization error system (6), the coupling delay $\tau(k)$ is assumed to be bounded within $[\tau_1, \tau_3]$. For a constant $\tau_2 \in [\tau_1, \tau_3]$, then either $\tau(k) \in [\tau_1, \tau_2]$ or $\tau(k) \in (\tau_2, \tau_3]$. The probabilities that $\tau(k)$ in the two intervals are defined as $\text{Prob}\{\tau(k) \in [\tau_1, \tau_2]\} = \bar{\beta}$ and $\text{Prob}\{\tau(k) \in (\tau_2, \tau_3]\} = 1 - \bar{\beta}$ $(0 \le \bar{\beta} \le 1)$. Then, we define a Bernoulli random variable to depict the characteristic of $\tau(k)$ as follows:

$$\beta(k) = \begin{cases} 1, \tau(k) \in [\tau_1, \tau_2] \\ 0, \tau(k) \in (\tau_2, \tau_3] \end{cases} \quad (7)$$

in which $\text{Prob}\{\beta(k) = 1\} = \bar{\beta}$, $\text{Prob}\{\beta(k) = 0\} = 1 - \bar{\beta}$. The probabilistic distribution of $\beta(k)$ can be obtained based on the statistical information derived by long-term monitoring on the coupling delay. According to the definition, $\tau(k)$ can be formulated as

$$\tau(k) = \begin{cases} \tau_1(k), \tau(k) \in [\tau_1, \tau_2] \\ \tau_2(k), \tau(k) \in (\tau_2, \tau_3] \end{cases} \quad (8)$$

where $\tau_1(k) = \beta(k)\tau(k)$ and $\tau_2(k) = (1-\beta(k))\tau(k)$.

Taking the above coupling delay into account, the synchronization error system model (6) can be updated as follows:

$$\begin{aligned} e_i(k+1) = {} & Ae_i(k) + Bg_i(k) + \sum_{j=1}^{N} \omega_{ij,q_i(k)} c_{ij} \Gamma_1 e_j(k) \\ & + \beta(k) \sum_{j=1}^{N} \omega_{ij,q_i(k)} c_{ij} \Gamma_2 e_j(k-\tau_1(k)) \\ & + (1-\beta(k)) \sum_{j=1}^{N} \omega_{ij,q_i(k)} c_{ij} \Gamma_2 e_j(k-\tau_2(k)) \\ & + Du_i(k). \end{aligned} \quad (9)$$

C. Asynchronous Deception Attacks

The synchronization controller for node$_i$ $(1 \le i \le N)$ under the described RR protocol in this article is designed as

$$u_i(k) = K_{i,\bar{q}_i(k)} e_i(k) \quad (10)$$

where $\bar{q}_i(k) = \text{mod}(k-1, Z) + 1$, and $K_{i,\bar{q}_i(k)}$ is the ideal controller gain which will be designed shortly.

Given that asynchronous deception attacks occurred on the N-CA is concerned, i.e., channel i is assumed to be attacked by DA_i, the actual signal arrived at actuator i can be described as

$$\hat{u}_i(k) = \alpha_i(k) h_i(u_i(k)) + (1-\alpha_i(k)) u_i(k) \quad (11)$$

where $\alpha_i(k)$ denotes a Bernoulli variable with $\text{Prob}\{\alpha_i(k) = 1\} = \bar{\alpha}_i$ $(\text{Prob}\{\alpha_i(k) = 0\} = 1 - \bar{\alpha}_i)$, $h_i(u_i(k))$ is the deception attack signal.

Assumption 2 [38]: It is supposed that $h_i(u_i(k))$ is bounded with the following condition:

$$\|h_i(u_i(k))\| \le \|G_i u_i(k)\| \quad (12)$$

where G_i is a known upper bound matrix of $h_i(\cdot)$.

Remark 3: Given that deception attacks can not always be launched successfully and then appear randomness, $\alpha_i(k)$ $(1 \le i \le N,\ k = 1, 2, \ldots)$ satisfies Bernoulli distribution is used to depict the occurrence of DA_i. To be specific, at time instant k, $\alpha_i(k) = 1$ indicates that the deception attack is occurred on channel i, and thus $u_i(k)$ is replaced by $h_i(u_i(k))$; otherwise, $\alpha_i(k) = 0$ denotes that $u_i(k)$ is transmitted from controller i to actuator i without the disturbing of the deception attack. Apparently, $\alpha_i(k)$ effectively reflects the stochastic feature of DA_i. Moreover, $h_i(.)$ with $\|h_i(u_i(k))\| \le \|G_i u_i(k)\|$ is adopted to model the attack signal due to the energy-bounded signals can not easily be detected. The upper bound G_i can be obtained by defender based on statistical information. Although the formulated attack signal may seem like a kind of nonlinear disturbance, but it has vastly different physical meaning.

By replacing the control input $u_i(k)$ formulated by (10) with the actual control signal $\hat{u}_i(k)$ given in (11), the synchronization error system model (9) can be further described as follows:

$$\begin{aligned} e_i(k+1) = {} & Ae_i(k) + Bg_i(k) + \sum_{j=1}^{N} \omega_{ij,q_i(k)} c_{ij} \Gamma_1 e_j(k) \\ & + \beta(k) \sum_{j=1}^{N} \omega_{ij,q_i(k)} c_{ij} \Gamma_2 e_j(k-\tau_1(k)) \\ & + (1-\beta(k)) \sum_{j=1}^{N} \omega_{ij,q_i(k)} c_{ij} \Gamma_2 e_j(k-\tau_2(k)) \\ & + (1-\alpha_i(k)) DK_{i,\bar{q}_i(k)} e_i(k) + \alpha_i(k) D h_i(u_i(k)). \end{aligned} \quad (13)$$

For the subsequent analysis, the augmented synchronization error system model is established as

$$\begin{aligned} e(k+1) = {} & \overline{A}e(k) + \overline{B}g(k) + W_{1,\overline{q}(k)} e(k) \\ & + \beta(k) W_{2,\overline{q}(k)} e(k-\tau_1(k)) \\ & + (1-\beta(k)) W_{2,\overline{q}(k)} e(k-\tau_2(k)) \\ & + (I-\alpha(k)) \overline{D} K_{\overline{q}(k)} e(k) + \alpha(k) \overline{D} h(u(k)) \end{aligned} \quad (14)$$

where

$$\begin{aligned} & e(k) = \text{col}_N\{e_i(k)\}, \overline{A} = \text{diag}\{A, A, \ldots, A\} \\ & g(k) = \text{col}_N\{g_i(k)\}, \overline{B} = \text{diag}\{B, B, \ldots, B\} \\ & W_{1,\overline{q}(k)} = \left[\omega_{ij,q_i(k)} c_{ij}\right]_{N \times N} \otimes \Gamma_1 \\ & W_{2,\overline{q}(k)} = \left[\omega_{ij,q_i(k)} c_{ij}\right]_{N \times N} \otimes \Gamma_2 \\ & \alpha(k) = \text{diag}\{\alpha_1(k), \alpha_2(k), \ldots, \alpha_N(k)\} \\ & e(k-\tau_1(k)) = \text{col}_N\{e_i(k-\tau_1(k))\} \\ & e(k-\tau_2(k)) = \text{col}_N\{e_i(k-\tau_2(k))\} \\ & \overline{D} = \text{diag}\{D, D, \ldots, D\}, h(u(k)) = \text{col}_N\{h_i(u_i(k))\} \\ & K_{\overline{q}(k)} = \text{diag}\{K_{1,\overline{q}_1(k)}, K_{2,\overline{q}_2(k)}, \ldots, K_{N,\overline{q}_N(k)}\} \\ & \overline{q}(k) = \text{mod}(k-1, Z) + 1. \end{aligned}$$

Based on (14), the synchronization control issue for the envisioned CN can be converted into assuring the stability of the augmented synchronization error system.

Before ending this section, the following lemmas are introduced to assist in achieving the major results of the study.

Lemma 1 [39]: Defining $y(k) = e(k+1) - e(k)$, for any matrix $Q > 0$, the following inequality holds:

$$-(\tau_2 - \tau_1) \sum_{s=k-\tau_2}^{k-\tau_1-1} y^T(s) Q y(s) \le \chi^T(k) \begin{bmatrix} -Q & Q \\ Q & -Q \end{bmatrix} \chi(k) \quad (15)$$

where $\chi(k) = \begin{bmatrix} e(k-\tau_1) \\ e(k-\tau_2) \end{bmatrix}$.

Lemma 2 [40]: For given ρ, $\varrho \in \mathbb{R}^{n_x}$, positive definite matrix Q, we have

$$2\rho^T \varrho \le \rho^T Q \rho + \varrho^T Q^{-1} \varrho. \quad (16)$$

Lemma 3 [41]: For $\tau_1 \le \tau(k) \le \tau_2$, and any constant matrices Ω_1, Ω_2 and Ω, the following inequality:

$$(\tau(k) - \tau_1)\Omega_1 + (\tau_2 - \tau(k))\Omega_2 + \Omega \le 0 \quad (17)$$

holds, if the two inequalities

$$(\tau_2 - \tau_1)\Omega_1 + \Omega \le 0, \quad (\tau_2 - \tau_1)\Omega_2 + \Omega \le 0$$

are satisfied.

III. Main Results

In this section, the sufficient conditions that guarantee the asymptotic stability of the established synchronization error system, i.e., the synchronization of the considered CN, are discussed in Theorem 1. Then, the controllers are designed accordingly in Theorem 2.

Theorem 1: For given positive scalars $\bar{\alpha}_i$ $(1 \le i \le N)$, $\bar{\beta}$, τ_1, τ_2, τ_3, ν_o, ι_o $(o = 1, 2, \dots, n_x)$, v $(v = 1, 2, 3, 4)$, and controllers gains matrices K_z $(z = 1, 2, \dots, Z)$, the asymptotic stability of the synchronization error system (14) can be achieved if there have positive definite matrices $P_z > 0$, $Q_a > 0$ $(a = 1, 2, 3)$, $R_a > 0$, $U > 0$, $G_i > 0$ and M, O, S, T with appropriate dimensions so that the nonlinear inequalities

$$\begin{bmatrix} \Xi_{1,z} & * & * & * & * \\ \Xi_{2,z} & \Xi_{6,z} & * & * & * \\ \Xi_{3,z} & 0 & \Xi_{7,z} & * & * \\ \Xi_{4,z} & 0 & 0 & -I & * \\ \Xi_5(v) & 0 & 0 & 0 & \Xi_8 \end{bmatrix} < 0 \quad (18)$$

hold, where

$$\Xi_{1,z} = \begin{bmatrix} \Phi_z + \Psi + \Psi^T & * \\ 0 & -I \end{bmatrix}, \ \Xi_{2,z} = \begin{bmatrix} \Xi_{21,z} & \Xi_{22,z} \end{bmatrix}$$

$$\Phi_z = \begin{bmatrix} \Pi_{1,z} & * & * & * & * & * & * \\ L_2 U & -U & * & * & * & * & * \\ R_1 & 0 & -Q_1 - R_1 & * & * & * & * \\ 0 & 0 & 0 & 0 & * & * & * \\ 0 & 0 & 0 & 0 & -Q_2 & * & * \\ 0 & 0 & 0 & 0 & 0 & 0 & * \\ 0 & 0 & 0 & 0 & 0 & 0 & -Q_3 \end{bmatrix}$$

$$\Psi = \begin{bmatrix} 0 & 0 & M & -M + O & -O + S & -S + T & -T \end{bmatrix}$$

$$\Xi_{3,z} = \begin{bmatrix} \Xi_{31,z} & \Xi_{32,z} \end{bmatrix}, \ \Xi_5(v) = \begin{bmatrix} \Xi_{51}(v) & 0 \end{bmatrix}$$

$$\Xi_{21,z} = \begin{bmatrix} \Pi_{2,z} & P_{z+1}\bar{B} & 0 & \Pi_{3,z} \\ 0 & 0 & 0 & \Pi_{4,z} \\ -\hat{\alpha} P_{z+1} \bar{D} K_z & 0 & 0 & 0 \end{bmatrix}$$

$$\Xi_{22,z} = \begin{bmatrix} 0 & \Pi_{5,z} & 0 & \bar{\alpha} P_{z+1} \bar{D} \\ 0 & \Pi_{6,z} & 0 & 0 \\ 0 & 0 & 0 & \hat{\alpha} P_{z+1} \bar{D} \end{bmatrix}$$

$$\Xi_{31,z} = \begin{bmatrix} \Pi_{7,z} & P_z \bar{B} & 0 & \bar{\beta} P_z W_{2,z} \\ 0 & 0 & 0 & \Pi_{8,z} \\ -\hat{\alpha} P_z \bar{D} K_z & 0 & 0 & 0 \end{bmatrix}$$

$$\Xi_{32,z} = \begin{bmatrix} 0 & \Pi_{9,z} & 0 & \bar{\alpha} P_z \bar{D} \\ 0 & \Pi_{10,z} & 0 & 0 \\ 0 & 0 & 0 & \hat{\alpha} P_z \bar{D} \end{bmatrix}$$

$$\Xi_{4,z} = \begin{bmatrix} G K_z & 0 & 0 & 0 & 0 & 0 & 0 & 0 \end{bmatrix}$$

$$\Xi_{51}(1) = \begin{bmatrix} \epsilon_1 M^T \\ \epsilon_2 S^T \end{bmatrix}, \ \Xi_{51}(2) = \begin{bmatrix} \epsilon_1 M^T \\ \epsilon_2 T^T \end{bmatrix}, \ \Xi_{51}(3) = \begin{bmatrix} \epsilon_1 O^T \\ \epsilon_2 S^T \end{bmatrix}$$

$$\Xi_{51}(4) = \begin{bmatrix} \epsilon_1 O^T \\ \epsilon_2 T^T \end{bmatrix}, \ G = \mathrm{diag}\{G_1, G_2, \dots, G_N\}$$

$$\begin{aligned}
\Xi_{6,z} &= \mathrm{diag}\{-P_{z+1}, -P_{z+1}, -P_{z+1}\} \\
\Xi_{7,z} &= \mathrm{diag}\{-P_z \Theta^{-1} P_z, -P_z \Theta^{-1} P_z, -P_z \Theta^{-1} P_z\} \\
\Xi_8 &= \mathrm{diag}\{-R_2, -R_3\} \\
\Theta &= \tau_1^2 R_1 + (\tau_2 - \tau_1) R_2 + (\tau_3 - \tau_2) R_3 \\
\Pi_{1,z} &= -P_z + Q_1 + Q_2 + Q_3 - R_1 - L_1 U \\
\Pi_{2,z} &= P_{z+1}\bar{A} + P_{z+1} W_{1,z} + \tilde{\alpha} P_{z+1} \bar{D} K_z \\
\Pi_{3,z} &= \bar{\beta} P_{z+1} W_{2,z}, \ \Pi_{4,z} = \hat{\beta} P_{z+1} W_{2,z} \\
\Pi_{5,z} &= \tilde{\beta} P_{z+1} W_{2,z}, \ \Pi_{6,z} = -\hat{\beta} P_{z+1} W_{2,z} \\
\Pi_{7,z} &= P_z\big(\bar{A} + W_{1,z} + \hat{\alpha} \bar{D} K_z - I\big) \\
\Pi_{8,z} &= \hat{\beta} P_z W_{2,z}, \ \Pi_{9,z} = \tilde{\beta} P_z W_{2,z} \\
\Pi_{10,z} &= -\hat{\beta} P_z W_{2,z}, \ \alpha = \mathrm{diag}\{\alpha_1, \alpha_2, \dots, \alpha_N\} \\
\tilde{\alpha} &= I - \bar{\alpha}, \ \hat{\alpha} = \sqrt{\bar{\alpha}(1 - \bar{\alpha})}, \ \tilde{\beta} = 1 - \bar{\beta}, \ \hat{\beta} = \sqrt{\bar{\beta}\big(1 - \bar{\beta}\big)} \\
L_1 &= I \otimes \bar{\iota}, L_2 = I \otimes \bar{\nu}, \bar{\iota} = \mathrm{diag}\{\iota_1 \nu_1, \iota_2 \nu_2, \dots, \iota_{n_x} \nu_{n_x}\} \\
\bar{\nu} &= \mathrm{diag}\left\{\frac{\iota_1 + \nu_1}{2}, \frac{\iota_2 + \nu_2}{2}, \dots, \frac{\iota_{n_x} + \nu_{n_x}}{2}\right\} \\
\epsilon_1 &= \sqrt{\tau_2 - \tau_1}, \epsilon_2 = \sqrt{\tau_3 - \tau_2}, P_{Z+1} = P_1.
\end{aligned}$$

Proof: In view of the system described by (14), we define a Lyapunov–Krsasovskii function $V(k)$ as

$$V(k) = V_1(k) + V_2(k) + V_3(k) \quad (19)$$

in which

$$V_1(k) = e^T(k) P_{\overline{q}(k)} e(k) \quad (20)$$

$$V_2(k) = \sum_{r=k-\tau_1}^{k-1} e^T(r) Q_1 e(r) + \sum_{r=k-\tau_2}^{k-1} e^T(r) Q_2 e(r) + \sum_{r=k-\tau_3}^{k-1} e^T(r) Q_3 e(r) \quad (21)$$

$$V_3(k) = \tau_1 \sum_{r=-\tau_1}^{-1} \sum_{s=k+r}^{k-1} \eta^T(s) R_1 \eta(s)$$

$$+\sum_{r=-\tau_2}^{-\tau_1-1}\sum_{s=k+r}^{k-1}\eta^T(s)R_2\eta(s)$$
$$+\sum_{r=-\tau_3}^{-\tau_2-1}\sum_{s=k+r}^{k-1}\eta^T(s)R_3\eta(s) \tag{22}$$

and $\eta(k) = e(k+1) - e(k)$, $P_{\overline{q}(k)} > 0$, $Q_a > 0$, $R_a > 0$ $(a = 1, 2, 3)$.

Denoting $\Delta V(k) = V(k+1) - V(k)$ and then taking the mathematical expectation of it, we can get

$$E\{\Delta V(k)\} = E\{\Delta V_1(k)\} + E\{\Delta V_2(k)\} + E\{\Delta V_3(k)\} \tag{23}$$

$$\begin{aligned} E\{\Delta V_1(k)\} &= E\{V_1(k+1) - V_1(k)\} \\ &= \mathcal{A}_1^T P_{\overline{q}(k+1)}\mathcal{A}_1 + \bar{\beta}\big(1-\bar{\beta}\big)\mathcal{B}_1^T P_{\overline{q}(k+1)}\mathcal{B}_1 \\ &\quad + \bar{\alpha}(I-\bar{\alpha})\mathcal{B}_2^T P_{\overline{q}(k+1)}\mathcal{B}_2 - e^T(k)P_{\overline{q}(k)}e(k) \end{aligned} \tag{24}$$

where

$$\begin{aligned} \mathcal{A}_1 &= \overline{A}e(k) + \overline{B}g(k) + W_{1,\overline{q}(k)}e(k) \\ &\quad + \bar{\beta}W_{2,\overline{q}(k)}e(k-\tau_1(k)) \\ &\quad + \big(1-\bar{\beta}\big)W_{2,\overline{q}(k)}e(k-\tau_2(k)) \\ &\quad + (I-\bar{\alpha})\overline{D}K_{\overline{q}(k)}e(k) + \bar{\alpha}\overline{D}h(u(k)) \\ \mathcal{B}_1 &= W_{2,\overline{q}(k)}e(k-\tau_1(k)) - W_{2,\overline{q}(k)}e(k-\tau_2(k)) \\ \mathcal{B}_2 &= \overline{D}h(u(k)) - \overline{D}K_{\overline{q}(k)}e(k) \end{aligned}$$

$$\begin{aligned} E\{\Delta V_2(k)\} &= E\{V_2(k+1) - V_2(k)\} \\ &= e^T(k)Q_1e(k) - e^T(k-\tau_1)Q_1e(k-\tau_1) \\ &\quad + e^T(k)Q_2e(k) - e^T(k-\tau_2)Q_2e(k-\tau_2) \\ &\quad + e^T(k)Q_3e(k) - e^T(k-\tau_3)Q_3e(k-\tau_3) \end{aligned} \tag{25}$$

$$\begin{aligned} E\{\Delta V_3(k)\} &= E\{V_3(k+1) - V_3(k)\} \\ &= -E\{\tau_1\sum_{r=k-\tau_1}^{k-1}\eta^T(r)R_1\eta(r)\} + E\{\eta^T(k)[\tau_1^2R_1 \\ &\quad + (\tau_2-\tau_1)R_2 + (\tau_3-\tau_2)R_3]\eta(k)\} \\ &\quad - E\{\sum_{r=k-\tau_2}^{k-\tau_1-1}\eta^T(r)R_2\eta(r)\} \\ &\quad - E\{\sum_{r=k-\tau_3}^{k-\tau_2-1}\eta^T(r)R_3\eta(r)\} \\ &\quad + E\{\gamma_1+\gamma_2+\gamma_3+\gamma_4\} \end{aligned} \tag{26}$$

where

$$\gamma_1 = 2\xi^T(k)M\left[e(k-\tau_1) - e(k-\tau_1(k)) - \sum_{r=k-\tau_1(k)}^{k-\tau_1-1}\eta(r)\right]$$
$$\gamma_2 = 2\xi^T(k)O\left[e(k-\tau_1(k)) - e(k-\tau_2) - \sum_{r=k-\tau_2}^{k-\tau_1(k)-1}\eta(r)\right]$$
$$\gamma_3 = 2\xi^T(k)S\left[e(k-\tau_2) - e(k-\tau_2(k)) - \sum_{r=k-\tau_2(k)}^{k-\tau_2-1}\eta(r)\right]$$
$$\gamma_4 = 2\xi^T(k)T\left[e(k-\tau_2(k)) - e(k-\tau_3) - \sum_{r=k-\tau_3}^{k-\tau_2(k)-1}\eta(r)\right]$$

$$\begin{aligned} \xi^T(k) = [&e^T(k), g^T(k), e^T(k-\tau_1), e^T(k-\tau_1(k)) \\ &e^T(k-\tau_2), e^T(k-\tau_2(k)), e^T(k-\tau_3)]. \end{aligned}$$

By employing Lemma 1, we can derive that

$$-\tau_1\sum_{r=k-\tau_1}^{k-1}\eta^T(r)R_1\eta(r) \le \chi^T(k)\begin{bmatrix}-R_1 & R_1\\ R_1 & -R_1\end{bmatrix}\chi(k) \tag{27}$$

where $\chi(k) = \begin{bmatrix}e(k)\\ e(k-\tau_1)\end{bmatrix}$. According to Lemma 2, it is obviously that

$$\begin{aligned} &-2\xi^T(k)M\sum_{r=k-\tau_1(k)}^{k-\tau_1-1}\eta(r) \\ &\le (\tau_1(k)-\tau_1)\xi^T(k)MR_2^{-1}M^T\xi(k) \\ &\quad + \sum_{r=k-\tau_1(k)}^{k-\tau_1-1}\eta^T(r)R_2\eta(r) \end{aligned} \tag{28}$$

$$\begin{aligned} &-2\xi^T(k)O\sum_{r=k-\tau_2}^{k-\tau_1(k)-1}\eta(r) \\ &\le (\tau_2-\tau_1(k))\xi^T(k)OR_2^{-1}O^T\xi(k) \\ &\quad + \sum_{r=k-\tau_2}^{k-\tau_1(k)-1}\eta^T(r)R_2\eta(r) \end{aligned} \tag{29}$$

$$\begin{aligned} &-2\xi^T(k)S\sum_{r=k-\tau_2(k)}^{k-\tau_2-1}\eta(r) \\ &\le (\tau_2(k)-\tau_2)\xi^T(k)SR_3^{-1}S^T\xi(k) \\ &\quad + \sum_{r=k-\tau_2(k)}^{k-\tau_2-1}\eta^T(r)R_3\eta(r) \end{aligned} \tag{30}$$

$$\begin{aligned} &-2\xi^T(k)T\sum_{r=k-\tau_3}^{k-\tau_2(k)-1}\eta(r) \\ &\le (\tau_3-\tau_2(k))\xi^T(k)TR_3^{-1}T^T\xi(k) + \sum_{r=k-\tau_3}^{k-\tau_2(k)-1}\eta^T(r)R_3\eta(r). \end{aligned} \tag{31}$$

Then, on the basis of (27)–(31), $E\{\Delta V_3(k)\}$ can be found to satisfy

$$\begin{aligned} E\{\Delta V_3(k)\} &\le \chi(k)^T\begin{bmatrix}-R_1 & R_1\\ R_1 & -R_1\end{bmatrix}\chi(k) \\ &\quad + \mathcal{A}_2^T\Theta\mathcal{A}_2 + \bar{\beta}\big(1-\bar{\beta}\big)\mathcal{B}_1^T\Theta\mathcal{B}_1 \\ &\quad + \bar{\alpha}(I-\bar{\alpha})\mathcal{B}_2^T\Theta\mathcal{B}_2 \\ &\quad + 2\xi^T(k)M[e(k-\tau_1) - e(k-\tau_1(k))] \\ &\quad + 2\xi^T(k)O[e(k-\tau_1(k)) - e(k-\tau_2)] \\ &\quad + 2\xi^T(k)S[e(k-\tau_2) - e(k-\tau_2(k))] \\ &\quad + 2\xi^T(k)T[e(k-\tau_2(k)) - e(k-\tau_3)] \\ &\quad + (\tau_1(k)-\tau_1)\xi^T(k)MR_2^{-1}M^T\xi(k) \\ &\quad + (\tau_2-\tau_1(k))\xi^T(k)OR_2^{-1}O^T\xi(k) \\ &\quad + (\tau_2(k)-\tau_2)\xi^T(k)SR_3^{-1}S^T\xi(k) \\ &\quad + (\tau_3-\tau_2(k))\xi^T(k)TR_3^{-1}T^T\xi(k) \end{aligned} \tag{32}$$

where $\mathcal{A}_2 = (\overline{A} + W_{1,\overline{q}(k)} - I)e(k) + \overline{B}g(k) + \bar{\beta}W_{2,\overline{q}(k)}e(k - \tau_1(k)) + \bar{\alpha}\overline{D}h(u(k)) + (1 - \bar{\beta})W_{2,\overline{q}(k)}e(k - \tau_2(k)) + (I - \bar{\alpha})\overline{D}K_{\overline{q}(k)}e(k)$.

Based on Assumption 1, we have

$$\begin{bmatrix} e(k) \\ g(k) \end{bmatrix}^T \begin{bmatrix} L_1 U & -L_2 U \\ -L_2 U & U \end{bmatrix} \begin{bmatrix} e(k) \\ g(k) \end{bmatrix} \leq 0. \tag{33}$$

Meanwhile, according to Assumption 2, we know that

$$h^T(u(k))h(u(k)) \leq u^T(k)G^T G u(k) \tag{34}$$

where $u(k) = \mathrm{col}_N\{u_i(k)\}$. Thus, by combining (24) and (25) and (32)–(34), it can be derived that

$$\begin{aligned} E\{\Delta V(k)\} \leq\ & \mathcal{A}_1^T P_{\overline{q}(k+1)} \mathcal{A}_1 + \bar{\beta}\big(1 - \bar{\beta}\big)\mathcal{B}_1^T P_{\overline{q}(k+1)} \mathcal{B}_1 \\ & + \bar{\alpha}(I - \bar{\alpha})\mathcal{B}_2^T P_{\overline{q}(k+1)} \mathcal{B}_2 - e^T(k) P_{\overline{q}(k)} e(k) \\ & + e^T(k) Q_1 e(k) - e^T(k - \tau_1) Q_1 e(k - \tau_1) \\ & + e^T(k) Q_2 e(k) - e^T(k - \tau_2) Q_2 e(k - \tau_2) \\ & + e^T(k) Q_3 e(k) - e^T(k - \tau_3) Q_3 e(k - \tau_3) \\ & + \chi(k)^T \begin{bmatrix} -R_1 & R_1 \\ R_1 & -R_1 \end{bmatrix} \chi(k) \\ & + \mathcal{A}_2^T \Theta \mathcal{A}_2 + \bar{\beta}\big(1 - \bar{\beta}\big)\mathcal{B}_1^T \Theta \mathcal{B}_1 \\ & + \bar{\alpha}(I - \bar{\alpha})\mathcal{B}_2^T \Theta \mathcal{B}_2 \\ & + 2\xi^T(k) M[e(k - \tau_1) - e(k - \tau_1(k))] \\ & + 2\xi^T(k) O[e(k - \tau_1(k)) - e(k - \tau_2)] \\ & + 2\xi^T(k) S[e(k - \tau_2) - e(k - \tau_2(k))] \\ & + 2\xi^T(k) T[e(k - \tau_2(k)) - e(k - \tau_3)] \\ & + (\tau_1(k) - \tau_1)\xi^T(k) M R_2^{-1} M^T \xi(k) \\ & + (\tau_2 - \tau_1(k))\xi^T(k) O R_2^{-1} O^T \xi(k) \\ & + (\tau_2(k) - \tau_2)\xi^T(k) S R_3^{-1} S^T \xi(k) \\ & + (\tau_3 - \tau_2(k))\xi^T(k) T R_3^{-1} T^T \xi(k) \\ & - \begin{bmatrix} e(k) \\ g(k) \end{bmatrix}^T \begin{bmatrix} L_1 U & -L_2 U \\ -L_2 U & U \end{bmatrix} \begin{bmatrix} e(k) \\ g(k) \end{bmatrix} \\ & + e^T(k) K_{\overline{q}(k)}^T G^T G K_{\overline{q}(k)} e(k) \\ & - h^T(u(k))h(u(k)). \end{aligned} \tag{35}$$

Therefore, based on Schur complement equivalence and Lemma 3, $E\{\Delta V(k)\} \leq 0$ can be guaranteed by (18), which means that the system (14) is asymptotically stable with the holding of (18). This completes the proof. ∎

As described in Theorem 1, the stability of the constructed system (14) is analyzed based on the given controllers gains and there exist nonlinear terms, e.g., $P_z \Theta^{-1} P_z$ ($z = 1, 2, \ldots, Z$), in (18) which makes it can hardly be computed. Thus, the method for designing appropriate controllers, i.e., the gains matrices K_z ($1 \leq z \leq Z$), based on handling the nonlinear terms is then presented by Theorem 2.

Theorem 2: For given positive scalars $\bar{\alpha}_i$ ($1 \leq i \leq N$), $\bar{\beta}$, τ_1, τ_2, τ_3, ν_o, ι_o ($o = 1, 2, \ldots, n_x$), κ, v ($v = 1, 2, 3, 4$), the asymptotic stability of the synchronization error system (14) can be achieved if there have positive definite matrices $X_z > 0$ ($z = 1, 2, \ldots, Z$), $\widetilde{Q_{a,z}} > 0$ ($a = 1, 2, 3$), $\widetilde{R_{a,z}} > 0$, $\widetilde{U_z} > 0$, $G > 0$, matrices $Y_z > 0$ and $\widetilde{M}_z$, $\widetilde{O}_z$, $\widetilde{S}_z$, $\widetilde{T}_z$ with appropriate dimensions to guarantee that the linear matrix inequalities (LMIs)

$$\begin{bmatrix} \widetilde{\Xi_{1,z}} & * & * & * & * \\ \widetilde{\Xi_{2,z}} & \widetilde{\Xi_{6,z}} & * & * & * \\ \widetilde{\Xi_{3,z}} & 0 & \widetilde{\Xi_{7,z}} & * & * \\ \widetilde{\Xi_{4,z}} & 0 & 0 & \Xi_8 & * \\ \widetilde{\Xi_{5,z}}(v) & 0 & 0 & 0 & \widetilde{\Xi_{9,z}} \end{bmatrix} < 0 \tag{36}$$

can be satisfied with controllers gains $K_z = Y_z X_z^{-1}$, where

$$\widetilde{\Xi_{1,z}} = \begin{bmatrix} \widetilde{\Phi_z} + \widetilde{\Psi_z} + \widetilde{\Psi_z}^T & * \\ 0 & -I \end{bmatrix}, \widetilde{\Xi_{2,z}} = \begin{bmatrix} \widetilde{\Xi_{21,z}} & \widetilde{\Xi_{22,z}} \end{bmatrix}$$

$$\widetilde{\Phi_z} = \begin{bmatrix} \widetilde{\Pi_{1,z}} & * & * & * & * & * & * \\ L_2\widetilde{U}_z & -\widetilde{U}_z & * & * & * & * & * \\ \widetilde{R_{1,z}} & 0 & \psi & * & * & * & * \\ 0 & 0 & 0 & 0 & * & * & * \\ 0 & 0 & 0 & 0 & -\widetilde{Q_{2,z}} & * & * \\ 0 & 0 & 0 & 0 & 0 & 0 & * \\ 0 & 0 & 0 & 0 & 0 & 0 & -\widetilde{Q_{3,z}} \end{bmatrix}$$

$$\widetilde{\Psi_z} = \begin{bmatrix} \widetilde{\Psi_{1,z}} & \widetilde{\Psi_{2,z}} \end{bmatrix}, \widetilde{\Psi_{1,z}} = \begin{bmatrix} 0 & 0 & \widetilde{M}_z \end{bmatrix}$$

$$\widetilde{\Psi_{2,z}} = \begin{bmatrix} -\widetilde{M}_z + \widetilde{O}_z & -\widetilde{O}_z + \widetilde{S}_z & -\widetilde{S}_z + \widetilde{T}_z & -\widetilde{T}_z \end{bmatrix}$$

$$\widetilde{\Xi_{3,z}} = \begin{bmatrix} \widetilde{\Xi_{31,z}} & \widetilde{\Xi_{32,z}} \end{bmatrix}, \widetilde{\Xi_{5,z}}(v) = \begin{bmatrix} \widetilde{\Xi_{51,z}}(v) & 0 \end{bmatrix}$$

$$\widetilde{\Xi_{21,z}} = \begin{bmatrix} \widetilde{\Pi_{2,z}} & \overline{B}X_z & 0 & \widetilde{\Pi_{3,z}} \\ 0 & 0 & 0 & \widetilde{\Pi_{4,z}} \\ -\hat{\alpha}\overline{D}Y_z & 0 & 0 & 0 \end{bmatrix}$$

$$\widetilde{\Xi_{22,z}} = \begin{bmatrix} 0 & \widetilde{\Pi_{5,z}} & 0 & \bar{\alpha}\overline{D} \\ 0 & \widetilde{\Pi_{6,z}} & 0 & 0 \\ 0 & 0 & 0 & \hat{\alpha}\overline{D} \end{bmatrix}$$

$$\widetilde{\Xi_{31,z}} = \begin{bmatrix} \widetilde{\Pi_{7,z}} & \overline{B}X_z & 0 & \bar{\beta}W_{2,z}X_z \\ 0 & 0 & 0 & \widetilde{\Pi_{8,z}} \\ -\hat{\alpha}\overline{D}K_z & 0 & 0 & 0 \end{bmatrix}$$

$$\widetilde{\Xi_{32,z}} = \begin{bmatrix} 0 & \widetilde{\Pi_{9,z}} & 0 & \bar{\alpha}\overline{D} \\ 0 & \widetilde{\Pi_{10,z}} & 0 & 0 \\ 0 & 0 & 0 & \hat{\alpha}\overline{D} \end{bmatrix}$$

$$\widetilde{\Xi_{4,z}} = \begin{bmatrix} 0 & 0 & 0 & \bar{\beta}GY_z & 0 & \tilde{\beta}GY_z & 0 & 0 \\ 0 & 0 & 0 & \hat{\beta}GY_z & 0 & -\hat{\beta}GY_z & 0 & 0 \end{bmatrix}$$

$$\widetilde{\Xi_{51,z}}(1) = \begin{bmatrix} \epsilon_1 \widetilde{M}_z^T \\ \epsilon_2 \widetilde{S}_z^T \end{bmatrix}, \widetilde{\Xi_{51,z}}(2) = \begin{bmatrix} \epsilon_1 \widetilde{M}_z^T \\ \epsilon_2 \widetilde{T}_z^T \end{bmatrix}$$

$$\widetilde{\Xi_{51,z}}(3) = \begin{bmatrix} \epsilon_1 \widetilde{O}_z^T \\ \epsilon_2 \widetilde{S}_z^T \end{bmatrix}, \widetilde{\Xi_{51,z}}(4) = \begin{bmatrix} \epsilon_1 \widetilde{O}_z^T \\ \epsilon_2 \widetilde{T}_z^T \end{bmatrix}$$

$$\begin{aligned} \widetilde{\Xi_{6,z}} &= \mathrm{diag}\{-X_{z+1}, -X_{z+1}, -X_{z+1}\} \\ \widetilde{\Xi_{7,z}} &= \mathrm{diag}\{-2\kappa X_z + \kappa^2\widetilde{\Theta}, -2\kappa X_z + \kappa^2\widetilde{\Theta} \\ &\quad - 2\kappa X_z + \kappa^2\widetilde{\Theta}\} \\ \widetilde{\Theta} &= \tau_1^2\widetilde{R_{1,z}} + (\tau_2 - \tau_1)\widetilde{R_{2,z}} + (\tau_3 - \tau_2)\widetilde{R_{3,z}} \\ \widetilde{\Xi_{9,z}} &= \mathrm{diag}\{-\widetilde{R_{2,z}}, -\widetilde{R_{3,z}}\}, \psi = -\widetilde{Q_{1,z}} - \widetilde{R_{1,z}} \\ \widetilde{\Pi_{1,z}} &= -X_z + \widetilde{Q_{1,z}} + \widetilde{Q_{2,z}} + \widetilde{Q_{3,z}} - \widetilde{R_{1,z}} - L_1\widetilde{U}_z \\ \widetilde{\Pi_{2,z}} &= \overline{A}X_z + W_{1,z}X_z + \tilde{\alpha}\overline{D}Y_z, \widetilde{\Pi_{3,z}} = \bar{\beta}W_{2,z}X_z \\ \widetilde{\Pi_{4,z}} &= \hat{\beta}W_{2,z}X_z, \widetilde{\Pi_{5,z}} = \tilde{\beta}W_{2,z}X_z, \widetilde{\Pi_{6,z}} = -\hat{\beta}W_{2,z}X_z \\ \widetilde{\Pi_{7,z}} &= \big(\overline{A} + W_{1,z} - I\big)X_z + \tilde{\alpha}\overline{D}Y_z, \widetilde{\Pi_{8,z}} = \hat{\beta}W_{2,z}X_z \\ \widetilde{\Pi_{9,z}} &= \tilde{\beta}W_{2,z}X_z, \widetilde{\Pi_{10,z}} = -\hat{\beta}W_{2,z}X_z, X_{Z+1} = X_1. \end{aligned}$$

Proof: For the given positive scalar κ, we can derive [42]

$$\left(R-\kappa^{-1}P\right)R^{-1}\left(R-\kappa^{-1}P\right)\geq 0 \tag{37}$$

where P and R are positive definite matrices. On the basis of (37), we can get

$$-PR^{-1}P\leq -2\kappa P+\kappa^2 R. \tag{38}$$

Thus, by substituting $-P_z\Theta^{-1}P_z$ with $-2\kappa P_z+\kappa^2\Theta$ in (18), we can obtain

$$\begin{bmatrix} \Xi_{1,z} & * & * & * & * \\ \Xi_{2,z} & \Xi_{6,z} & * & * & * \\ \Xi_{3,z} & 0 & \overline{\Xi_{7,z}} & * & * \\ \Xi_{4,z} & 0 & 0 & -I & * \\ \Xi_5(v) & 0 & 0 & 0 & \Xi_8 \end{bmatrix}<0 \tag{39}$$

where $\overline{\Xi_{7,z}}=\text{diag}\{-2\kappa P_z+\kappa^2\Theta,-2\kappa P_z+\kappa^2\Theta,-2\kappa P_z+\kappa^2\Theta\}$.

Defining $X_z=P_z^{-1}$, $Y_z=K_zX_z$, $J=\text{diag}\{X_z,X_z,X_z,X_z,X_z,X_z,X_z,I,X_{z+1},X_{z+1},X_{z+1},X_z,X_z,X_z,I,X_z,X_z\}$, $\widetilde{Q}_{a,z}=X_z^TQ_aX_z$, $\widetilde{R}_{a,z}=X_z^TR_aX_z$, $\widetilde{M}_z=X_z^TMX_z$, $\widetilde{O}_z=X_z^TOX_z$, $\widetilde{S}_z=X_z^TSX_z$, $\widetilde{T}_z=X_z^TTX_z$, $\widetilde{U}_z=X_z^TUX_z$. Then, (36) can be derived by multiplying (39) on both sides with J and recurring to Schur complement. Therefore, the theorem can be obtained. ■

Remark 4: It is worthy noting that the LMIs presented in Theorem 2 may seem complicated, but the gains matrices of each controller i $(1\leq i\leq N)$ will be calculated in a decentralized manner, then the computation complexity of LMIs can be reduced effectively. Furthermore, with the enhancement of local computing capability of each node$_i$, and with the aid of edge computing and cloud computing, it is foreseeable that the computation of the LMIs will not result in high conservativeness of the presented main results.

Remark 5: The synchronization issue for CNs has gained widely attention, and some of reported researches are closely relevant with our study. For the related works that using RR protocol to avoid data conflict introduced by limited communication bandwidth of CNs, such as [15], [16], and [43], however, they all focus on designing appropriate estimators for CNs, rather than realizing the synchronization of CNs which is the objective of our study. Taking the probabilistic coupling delay into account, some synchronization methods have been proposed in recent literatures [21], [22], nevertheless, the works neglect the influence of the constrained communication resources on the signal transmission among CN nodes, so our designed synchronization approach differs greatly from such related methods. Focusing on CNs that the N-CA channels are compromised by asynchronous deception attacks, the secure synchronization problem has been investigated in the existed researches [34], [44], but comparing with our study, the impact of probabilistic coupling delay did not be considered in [34] and different deception attack model is adopted in [44], moreover, none of the two works employs RR protocol for conflict-free data exchange among CN nodes.

IV. Numerical Experiments

In this section, two experiments are conducted to illustrate the effectiveness of the developed synchronization control strategy for the envisioned CN. The one focuses on the CN with complete graph topology which means that all c_{ij} $(1\leq i\neq j\leq N)$ are larger than zero. The other concentrates on the CN with noncomplete graph topology, i.e., there exist some c_{ij} that equal to zero.

A. CN With Complete Graph Topology

Considering a discrete-time CN (1) with three nodes (i.e., N = 3) that represents an interconnected flexible link robot system [45], where the state of each node$_i$ can be denoted as $x_i(k)=\begin{bmatrix}x_{i1}(k) & x_{i2}(k) & x_{i3}(k) & x_{i4}(k)\end{bmatrix}^T$ by using $x_{i1}(k)$, $x_{i2}(k)$, $x_{i3}(k)$ and $x_{i4}(k)$ to indicate the angular position and velocity of the motor shaft, the angular position and velocity of the link, respectively. The system parameters are defined as follows:

$$A=\begin{bmatrix} -0.0727 & 0.0002 & 0.2095 & -0.0240 \\ -0.4842 & -0.0751 & 1.2996 & 0.2095 \\ -0.0362 & -0.0098 & 0.2351 & 0.0562 \\ 1.5873 & -0.0852 & -3.4969 & 0.2351 \end{bmatrix}$$

$$B=\text{diag}\{0.1,0.1,0.1,0.1\},\ \Gamma_1=\text{diag}\{0.5,0.5,0.6,0.6\}$$

$$\Gamma_2=\text{diag}\{0.6,0.6,0.5,0.5\},\ D=\text{col}\{0.1,-0.1,0.1,-0.1\}.$$

The coupling matrix of the three nodes is set to be

$$C=\begin{bmatrix} -0.2 & 0.1 & 0.1 \\ 0.1 & -0.2 & 0.1 \\ 0.1 & 0.1 & -0.2 \end{bmatrix} \tag{40}$$

which reveals the complete graph topology of the CN. By referring to [13], the nonlinear function is defined as

$$f(x_i(k))=\begin{bmatrix} 0.1\zeta_{i1}(k)-0.1\tanh(\zeta_{i2}(k)) \\ 0.1\zeta_{i2}(k)-0.3\tanh(\zeta_{i1}(k)) \end{bmatrix},\ i=1,2,3 \tag{41}$$

where $\zeta_{i1}(k)=\text{col}\{x_{i1}(k),x_{i2}(k)\}$ and $\zeta_{i2}(k)=\text{col}\{x_{i3}(k),x_{i4}(k)\}$.

The time delay $\tau(k)$ is assumed to be in the set [1, 10] and the distribution follows the probability of $\bar{\beta}=0.7$ with $\tau_2=5$. For the deception attacks, we define $\bar{\alpha}_1=0.7$, $\bar{\alpha}_2=0.5$, $\bar{\alpha}_3=0.3$, and set $h_i(u_i(t))$ $(i=1,2,3)$ as [34]

$$h_i(u_i(k))=0.1u_i(k)+\tanh(0.1u_i(k)) \tag{42}$$

with the upper bound matrix $G_i=0.2$. By further determining $\kappa=1$, $p_1(0)=2$, $p_2(0)=1$, $p_3(0)=2$, and calculating the LMIs (36) shown in Theorem 2, we can obtain the controllers gains matrices $K_{i,z}$ $(i=1,2,3,\ z=1,2)$ as listed in Table I.

We then set the state initial conditions of the isolated node and subsystems as $s(0)=\begin{bmatrix}0.5 & 1 & 0 & 0\end{bmatrix}^T$, $x_1(0)=\begin{bmatrix}-1 & 0.25 & 0 & 0\end{bmatrix}^T$, $x_2(0)=\begin{bmatrix}0.1 & 0 & 0.5 & 0\end{bmatrix}^T$, $x_3(0)=\begin{bmatrix}-0.5 & 0.25 & 0 & 1\end{bmatrix}^T$, based on which, the simulation results are specifically shown in Figs. 2–5.

Figs. 2 and 3 depict the responses of synchronization errors and the system states, respectively. We can find that the synchronization errors eventually converge to zero as presented in Fig. 2, and the system states become stable after about 20 time instants as shown in Fig. 3. Both of which fully validate the effectiveness of the designed synchronization control approach. Fig. 4 describes the trajectory of the considered coupling delay. As shown, most of the values of the coupling

TABLE I
PARAMETERS $K_{i,z}$, $(i = 1, 2, 3, z = 1, 2)$

$K_{i,z}$		$z = 1$
$i = 1$	$K_{1,1} =$	$\begin{bmatrix} -0.9870 & -0.1937 & 2.0190 & -0.3237 \end{bmatrix}$
$i = 2$	$K_{2,1} =$	$\begin{bmatrix} -1.5488 & -0.2718 & 3.1845 & -0.4714 \end{bmatrix}$
$i = 3$	$K_{3,1} =$	$\begin{bmatrix} -2.1083 & -0.3047 & 4.3016 & -0.5810 \end{bmatrix}$
$K_{i,z}$		$z = 2$
$i = 1$	$K_{1,2} =$	$\begin{bmatrix} -0.7025 & -0.2430 & 1.4489 & -0.3215 \end{bmatrix}$
$i = 2$	$K_{2,2} =$	$\begin{bmatrix} -0.9737 & -0.3046 & 1.9458 & -0.4340 \end{bmatrix}$
$i = 3$	$K_{3,2} =$	$\begin{bmatrix} -1.3611 & -0.3197 & 2.6150 & -0.5452 \end{bmatrix}$

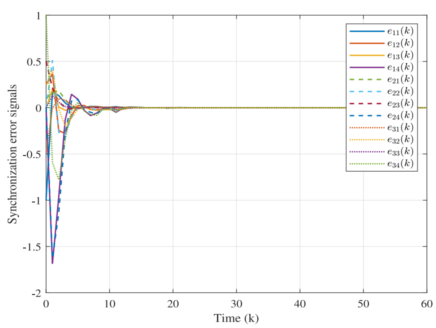

Fig. 2. Trajectories of $e_i(k)$ $(i = 1, 2, 3)$.

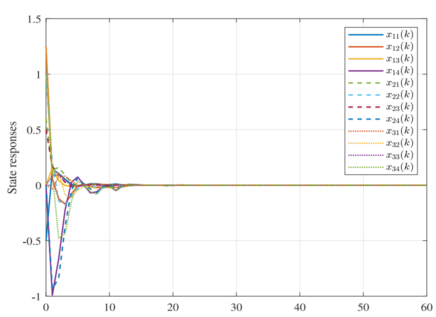

Fig. 3. Trajectories of $x_i(k)$ $(i = 1, 2, 3)$.

delay are distributed in the interval $[1, 5]$ given that $\bar{\beta}$ is set to be 0.7. Furthermore, Fig. 5 presents the occurrence of the deception attacks that asynchronously aimed at the N-CA in the simulated system.

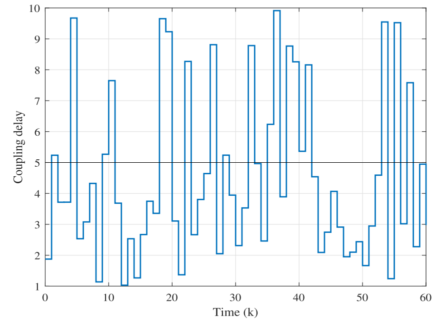

Fig. 4. Probabilistic interval coupling delay $\tau(k)$.

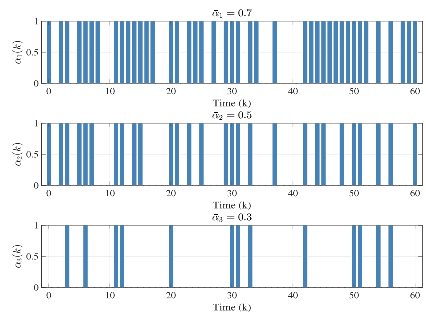

Fig. 5. Occurrence of deception attacks $\alpha_i(k)$ $(i = 1, 2, 3)$.

B. CN With Noncomplete Graph Topology

Considering a discrete-time CN system (1) consists of four nodes (i.e., $N = 4$) with noncomplete graph topology, the coupling matrix is set as

$$C = \begin{bmatrix} -0.2 & 0.1 & 0 & 0.1 \\ 0.1 & -0.3 & 0.1 & 0.1 \\ 0 & 0.1 & -0.1 & 0 \\ 0.1 & 0.1 & 0 & -0.2 \end{bmatrix}. \qquad (43)$$

Let $x_i(k) = \left[x_{i1}(k)\ x_{i2}(k)\right]^T$ $(i = 1, 2, 3, 4)$, then the nonlinear function $f(.)$ is defined similar to that in (41) by replacing ζ_{il} with x_{il} $(l = 1, 2)$, respectively.

The system parameters are set as follows according to [43]:

$$A = \begin{bmatrix} 0.42 & -0.51 \\ -0.26 & 0.45 \end{bmatrix}, B = \begin{bmatrix} 0.1 & 0.1 \\ 0 & 0.15 \end{bmatrix}, \Gamma_1 = \begin{bmatrix} 0.5 & 0 \\ 0 & 0.6 \end{bmatrix}$$
$$\Gamma_2 = \begin{bmatrix} 0.6 & 0 \\ 0 & 0.5 \end{bmatrix}, D = \begin{bmatrix} 0.1 \\ 0.1 \end{bmatrix}.$$

The probabilistic interval coupling delay is the same as that in the first experiment, the attack signals are also generated based on (42). Setting $\bar{\alpha}_1 = 0.7$, $\bar{\alpha}_2 = 0.5$, $\bar{\alpha}_3 = 0.3$, $\bar{\alpha}_4 = 0.6$, $\kappa = 1$, $p_1(0) = 2$, $p_2(0) = 3$, $p_3(0) = 1$, and $p_4(0) = 2$, then, the calculated $K_{i,z}$ $(i = 1, 2, 3, 4,\ z = 1, 2, 3, 4, 5, 6)$ in the experiment are listed in Table II.

By further setting the initial states of the isolated node and four CN nodes to be $s(0) = \left[-10.5\ 10.5\right]^T$, $x_1(0) = \left[20.5\ -10.5\right]^T$, $x_2(0) = \left[15\ -20.5\right]^T$, $x_3(0) = \left[5.6\ -15.2\right]^T$, $x_4(0) = \left[-11.6\ 25.2\right]^T$, and running the proposed synchronization control method, the final results are then presented with Figs. 6–9. To be specific, the responses of synchronization errors and the trajectories of system states are shown in Figs. 6 and 7, respectively. The feasibility of the proposed synchronization control approach is further validated by the two figures. The distribution of the asynchronous deception attacks is described by Fig. 8. The synchronization errors

TABLE II
PARAMETERS $K_{i,z}$, $(i = 1, 2, 3, 4, z = 1, 2, 3, 4, 5, 6)$

$K_{i,z}$	$z = 1$	$z = 2$
$i = 1$	$K_{1,1} = \begin{bmatrix} -0.0602 & 0.0810 \end{bmatrix}$	$K_{1,2} = \begin{bmatrix} -0.0747 & 0.1105 \end{bmatrix}$
$i = 2$	$K_{2,1} = \begin{bmatrix} -0.1162 & 0.1714 \end{bmatrix}$	$K_{2,2} = \begin{bmatrix} -0.1606 & 0.2519 \end{bmatrix}$
$i = 3$	$K_{3,1} = \begin{bmatrix} -0.1271 & 0.2136 \end{bmatrix}$	$K_{3,2} = \begin{bmatrix} -0.1552 & 0.2643 \end{bmatrix}$
$i = 4$	$K_{4,1} = \begin{bmatrix} -0.0783 & 0.1268 \end{bmatrix}$	$K_{4,2} = \begin{bmatrix} -0.1106 & 0.1807 \end{bmatrix}$
$K_{i,z}$	$z = 3$	$z = 4$
$i = 1$	$K_{1,3} = \begin{bmatrix} -0.0619 & 0.1001 \end{bmatrix}$	$K_{1,4} = \begin{bmatrix} -0.0585 & 0.0929 \end{bmatrix}$
$i = 2$	$K_{2,3} = \begin{bmatrix} -0.1416 & 0.2291 \end{bmatrix}$	$K_{2,4} = \begin{bmatrix} -0.1379 & 0.2217 \end{bmatrix}$
$i = 3$	$K_{3,3} = \begin{bmatrix} -0.1388 & 0.2459 \end{bmatrix}$	$K_{3,4} = \begin{bmatrix} -0.1411 & 0.2479 \end{bmatrix}$
$i = 4$	$K_{4,3} = \begin{bmatrix} -0.0966 & 0.1613 \end{bmatrix}$	$K_{4,4} = \begin{bmatrix} -0.0921 & 0.1533 \end{bmatrix}$
$K_{i,z}$	$z = 5$	$z = 6$
$i = 1$	$K_{1,5} = \begin{bmatrix} -0.0563 & 0.0888 \end{bmatrix}$	$K_{1,6} = \begin{bmatrix} -0.0601 & 0.0938 \end{bmatrix}$
$i = 2$	$K_{2,5} = \begin{bmatrix} -0.1276 & 0.2048 \end{bmatrix}$	$K_{2,6} = \begin{bmatrix} -0.1221 & 0.1950 \end{bmatrix}$
$i = 3$	$K_{3,5} = \begin{bmatrix} -0.1388 & 0.2357 \end{bmatrix}$	$K_{3,6} = \begin{bmatrix} -0.1217 & 0.2162 \end{bmatrix}$
$i = 4$	$K_{4,5} = \begin{bmatrix} -0.0914 & 0.1544 \end{bmatrix}$	$K_{4,6} = \begin{bmatrix} -0.0829 & 0.1349 \end{bmatrix}$

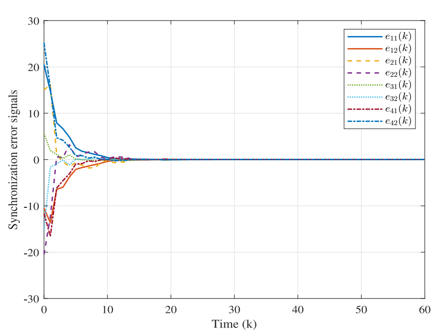

Fig. 6. Trajectories of $e_i(k)$ $(i = 1, 2, 3, 4)$.

obtained with and without the deception attacks are further presented in Fig. 9. It can be found that $||e(k)||$ derived with the deception attacks is larger than that obtained under the nonattack scenario, which reveals the influence of the deception attacks on system performance. It is also worth noting that $||e(k)||$ will tend to zero even under the deception attacks, which further confirms the efficiency of the devised synchronization control method.

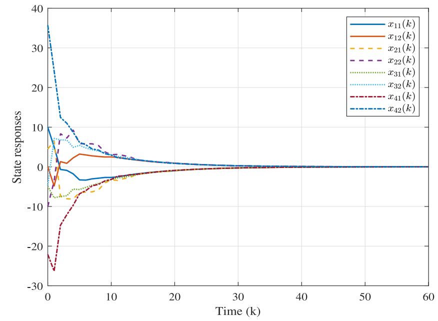

Fig. 7. Trajectories of $x_i(k)$ $(i = 1, 2, 3, 4)$.

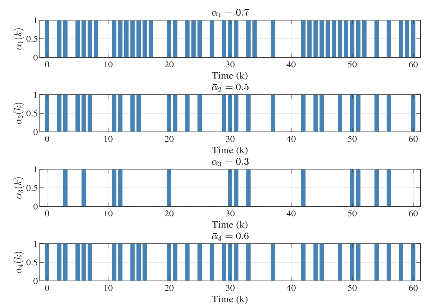

Fig. 8. Occurrence of deception attacks $\alpha_i(k)$ $(i = 1, 2, 3, 4)$.

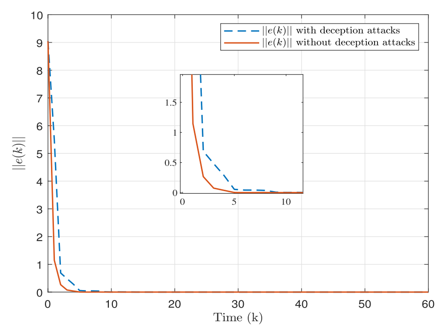

Fig. 9. $||e(k)||$ obtained with and without the deception attacks.

V. CONCLUSION

In this article, for a discrete-time CN with crowded, delayed internode communication network and vulnerable N-CA, a synchronization control method has been proposed to assure the desired performance of the considered system. Focusing on the internode communication network, RR protocol has been introduced to efficiently schedule nodes that generate traffic with the same destination; meanwhile, the time-vary and burstiness of the coupling delay have been well depicted by a probabilistic interval model driven by a Bernoulli parameter. For the sliced N-CA, the deception attack occurred on each of channels has been independently modeled by a different Bernoulli process. Based on the formal description of the considered scenario, a novel synchronization error model for the CN has been constructed. Then, decentralized controllers have been designed by recurring to Lyapunov stability theory and LMI technique. Simulation results obtained over CNs with complete and noncomplete graph topologies have illustrated the performance of the proposed synchronization strategy.

In future work, we will take into consideration of multichannel internode communication network, based on which each node in CNs can receive signals from multiple neighbors at each time instant, and then explore the security synchronization control for CNs with multichannel oriented RR protocol.

REFERENCES

[1] Q. Cai, S. Alam, M. Pratama, and J. Liu, "Robustness evaluation of multipartite complex networks based on percolation theory," *IEEE Trans. Syst., Man, Cybern., Syst.*, vol. 51, no. 10, pp. 6244–6257, Oct. 2021.

[2] D. Yang, Y. Sun, Q. Wei, H. Zhang, and T. Li, "Topology prediction and structural controllability analysis of complex networks without connection information," *IEEE Trans. Syst., Man, Cybern., Syst.*, vol. 52, no. 9, pp. 6015–6027, Sep. 2022.

[3] H. Que, M. Fang, Z. Wu, H. Su, T. Huang, and D. Zhang, "Exponential Synchronization via aperiodic sampling of complex delayed networks," *IEEE Trans. Syst., Man, Cybern., Syst.*, vol. 49, no. 7, pp. 1399–1407, Jul. 2019.

[4] Z. Tang, J. H. Park, Y. Wang, and J. Feng, "Adaptively Synchronize the derivative coupled complex networks with proportional delay," *IEEE Trans. Syst., Man, Cybern., Syst.*, vol. 51, no. 8, pp. 4969–4979, Aug. 2021.

[5] J. Hu, G. Sui, and X. Li, "Fixed-time synchronization of complex networks with time-varying delays," *Chaos, Solitons Fractals*, vol. 140, pp. 1–13, Nov. 2020.

[6] X. He and H. Zhang, "Exponential synchronization of complex networks via feedback control and periodically intermittent noise," *J. Frankl. Inst.*, vol. 359, no. 8, pp. 3614–3630, 2022.

[7] L. V. Gambuzza, M. Frasca, and V. Latora, "Distributed control of synchronization of a group of network nodes," *IEEE Trans. Autom. Control*, vol. 64, no. 1, pp. 365–372, Jan. 2019.

[8] P. Feketa, A. Schaum, and T. Meurer, "Synchronization and multicluster capabilities of oscillatory networks with adaptive coupling," *IEEE Trans. Autom. Control*, vol. 66, no. 7, pp. 3084–3096, Jul. 2021.

[9] B. Li, Z. Wang, and L. Ma, "An event-triggered pinning control approach to Synchronization of discrete-time stochastic complex dynamical networks," *IEEE Trans. Neural Netw. Learn. Syst.*, vol. 29, no. 12, pp. 5812–5822, Dec. 2018.

[10] Q. Li, B. Shen, Z. Wang, T. Huang, and J. Luo, "Synchronization control for a class of discrete time-delay complex dynamical networks: A dynamic event-triggered approach," *IEEE Trans. Cybern.*, vol. 49, no. 5, pp. 1979–1986, May 2019.

[11] Z. Hu, F. Deng, and Z. Wu, "Synchronization of stochastic complex dynamical networks subject to consecutive packet dropouts," *IEEE Trans. Cybern.*, vol. 51, no. 7, pp. 3779–3788, Jul. 2021.

[12] J. Wang, Z. Qin, H. Wu, and T. Huang, "Finite-time synchronization and H_∞ synchronization of multiweighted complex networks with adaptive state couplings," *IEEE Trans. Cybern.*, vol. 50, no. 2, pp. 600–612, Feb. 2020.

[13] Y. Li, F. Song, J. Liu, X. Xie, and E. Tian, "Decentralized event-triggered synchronization control for complex networks with nonperiodic DoS attacks," *Int. J. Robust Nonlin. Control*, vol. 32, no. 3, pp. 1633–1653, 2022.

[14] J. Liu, E. Gong, L. Zha, X. Xie, and E. Tian, "Outlier-resistant recursive security filtering for multirate networked systems under fading measurements and round robin protocol," *IEEE Trans. Control Netw. Syst.*, vol. 10, no. 4, pp. 1962–1974, Dec. 2023.

[15] X. Wan, Z. Wang, M. Wu, and X. Liu, "H_∞ state estimation for discrete-time nonlinear singularly perturbed complex networks under the round robin protocol," *IEEE Trans. Neural Netw. Learn. Syst.*, vol. 30, no. 2, pp. 415–426, Feb. 2019.

[16] D. Liu, Z. Wang, Y. Liu, F. E. Alsaadi, and F. E. Alsaadi, "Recursive state estimation for stochastic complex networks under round robin communication protocol: Handling packet disorders," *IEEE Trans. Netw. Sci. Eng.*, vol. 8, no. 3, pp. 2455–2468, Sep. 2021.

[17] M. Park, S. Lee, O. Kwon, and A. Seuret, "Closeness-centrality-based synchronization criteria for complex dynamical networks with interval time-varying coupling delays," *IEEE Trans. Cybern.*, vol. 48, no. 7, pp. 2192–2202, Jul. 2018.

[18] X. Lv, J. Cao, X. Li, M. Abdelaty, and U. A. Aljuboori, "Synchronization analysis for complex dynamical networks with coupling delay via event-triggered delayed impulsive control," *IEEE Trans. Cybern.*, vol. 51, no. 11, pp. 5269–5278, Nov. 2021.

[19] R. Sakthivel, R. Sakthivel, F. Alzahrani, P. Selvaraj, and S. M. Anthoni, "Synchronization of complex dynamical networks with random coupling delay and actuator faults," *ISA Trans.*, vol. 94, pp. 57–69, Nov. 2019.

[20] R. Cheng, M. Peng, J. Yu, and H. Li, "Synchronization for discrete-time complex networks with probabilistic time delays," *Physica A Stat. Mech. Appl.*, vol. 525, pp. 1088–1101, Jul. 2019.

[21] H. Bao, J. H. Park, and J. Cao, "Exponential Synchronization of coupled stochastic Memristor-based neural networks with time-varying probabilistic delay coupling and impulsive delay," *IEEE Trans. Neural Netw. Learn. Syst.*, vol. 27, no. 1, pp. 190–201, Jan. 2016.

[22] Y. Ren, H. Jiang, J. Li, and B. Lu, "Finite-time synchronization of stochastic complex networks with random coupling delay via quantized aperiodically intermittent control," *Neurocomputing*, vol. 420, pp. 337–348, Jan. 2021.

[23] L. Ding, Q. Han, B. Ning, and D. Yue, "Distributed resilient finite-time secondary control for heterogeneous battery energy storage systems under denial-of-service attacks," *IEEE Trans. Ind. Informat.*, vol. 16, no. 7, pp. 4909–4919, Jul. 2020.

[24] X. Wang, E. Tian, B. Wei, and J. Liu, "Novel attack-defense framework for nonlinear complex networks: An important-data-based method," *Int. J. Robust Nonlin. Control*, vol. 33, no. 4, pp. 2861–2878, 2022.

[25] M. Ye, D. Li, Q. Han, and L. Ding, "Distributed Nash equilibrium seeking for general networked games with bounded disturbances," *IEEE/CAA J. Automatica Sinica*, vol. 10, no. 2, pp. 376–387, Feb. 2023.

[26] X. Xu, X. Li, P. Dong, Y. Liu, and H. Zhang, "Robust reset speed Synchronization control for an integrated motor-transmission powertrain system of a connected vehicle under a replay attack," *IEEE Trans. Veh. Technol.*, vol. 70, no. 6, pp. 5524–5536, Jun. 2021.

[27] Y. Yu, W. Yang, W. Ding, and J. Zhou, "Reinforcement learning solution for cyber-physical systems security against replay attacks," *IEEE Trans. Inf. Forensics Security*, vol. 18, pp. 2583–2595, 2023.

[28] Y. Ma, W. Che, and C. Deng, "Dynamic event-triggered model-free adaptive control for nonlinear CPSs under aperiodic DoS attacks," *Inf. Sci.*, vol. 589, pp. 790–801, Apr. 2022.

[29] E. Tian, H. Chen, C. Wang, and L. Wang, "Security-ensured state of charge estimation of lithium-ion batteries subject to malicious attacks," *IEEE Trans. Smart Grid*, vol. 14, no. 3, pp. 2250–2261, May 2023.

[30] Z. Gu, T. Yin, and Z. Ding, "Path tracking control of autonomous vehicles subject to deception attacks via a learning-based event-triggered mechanism," *IEEE Trans. Neural Netw. Learn. Syst.*, vol. 32, no. 12, pp. 5644–5653, Dec. 2021.

[31] L. Zha, R. Liao, J. Liu, X. Xie, E. Tian, and J. Cao, "Dynamic event-triggered output feedback control for networked systems subject to multiple cyber attacks," *IEEE Trans. Cybern.*, vol. 52, no. 12, pp. 13800–13808, Dec. 2022.

[32] Z. Gu, P. Shi, D. Yue, S. Yan, and X. Xie, "Memory-based continuous event-triggered control for networked T–S fuzzy systems against cyberattacks," *IEEE Trans. Fuzzy Syst.*, vol. 29, no. 10, pp. 3118–3129, Oct. 2021.

[33] Y. Yang, J. Huang, X. Su, K. Wang, and G. Li, "Adaptive control of second-order nonlinear systems with injection and deception attacks," *IEEE Trans. Syst., Man, Cybern., Syst.*, vol. 52, no. 1, pp. 574–581, Jan. 2022.

[34] R. Pan, Y. Tan, D. Du, and S. Fei, "Adaptive event-triggered synchronization control for complex networks with quantization and cyber-attacks," *Neurocomputing*, vol. 382, pp. 249–258, Mar. 2020.

[35] B. Shen, Z. Wang, D. Wang, and Q. Li, "State-saturated recursive filter design for stochastic time-varying nonlinear complex networks under deception attacks," *IEEE Trans. Neural Netw. Learn. Syst.*, vol. 31, no. 10, pp. 3788–3800, Oct. 2020.

[36] N. Rong and Z. Wang, "Event-based impulsive control of IT2 T–S fuzzy interconnected system under deception attacks," *IEEE Trans. Fuzzy Syst.*, vol. 29, no. 6, pp. 1615–1628, Jun. 2021.

[37] Z. Zhao, Z. Wang, L. Zou, and G. Guo, "Finite-time state estimation for delayed neural networks with redundant delayed channels," *IEEE Trans. Syst., Man, Cybern., Syst.*, vol. 51, no. 1, pp. 441–451, Jan. 2021.

[38] F. Qu, E. Tian, and X. Zhao, "Chance-constrained H_∞ state estimation for recursive neural networks under deception attacks and energy constraints: The finite-horizon case," *IEEE Trans. Neural Netw. Learn. Syst.*, vol. 34, no. 9, pp. 6492–6503, Sep. 2023.

[39] Y. Chen, Z. Wang, S. Fei, and Q. Han, "Regional Stabilization for discrete time-delay systems with actuator saturations via a delay-dependent polytopic approach," *IEEE Trans. Autom. Control*, vol. 64, no. 3, pp. 1257–1264, Mar. 2019.

[40] J. Liu, Z. Wu, D. Yue, and J. H. Park, "Stabilization of networked control systems with hybrid-driven mechanism and probabilistic cyber attacks," *IEEE Trans. Syst., Man, Cybern., Syst.*, vol. 51, no. 2, pp. 943–953, Feb. 2021.

[41] E. Tian, D. Yue, and Y. Zhang, "Delay-dependent robust H_∞ control for T–S fuzzy system with interval time-varying delay," *Fuzzy Sets Syst.*, vol. 160, no. 12, pp. 1708–1719, Aug. 2009.

[42] J. Liu, Y. Wang, J. Cao, D. Yue, and X. Xie, "Secure adaptive-event-triggered filter design with input constraint and hybrid cyber attack," *IEEE Trans. Cybern.*, vol. 51, no. 8, pp. 4000–4010, Aug. 2021.

[43] M. Gao, W. Zhang, L. Sheng, and D. Zhou, "Distributed fault estimation for delayed complex networks with round robin protocol based on unknown input observer," *J. Frankl. Inst.*, vol. 357, no. 13, pp. 8678–8702, 2020.

[44] N. Sakthivel, "Synchronization of complex dynamical networks subjected to actuator faults and periodic scaling attacks using probabilistic time-varying delays," *Chaos, Solitons Fractals*, vol. 171, pp. 1–12, Jun. 2023.

[45] S. Wang, Z. Wang, H. Dong, and Y. Chen, "A dynamic event-triggered approach to recursive nonfragile filtering for complex networks with sensor saturations and switching topologies," *IEEE Trans. Cybern.*, vol. 52, no. 10, pp. 11041–11054, Oct. 2022.

Yan Li received the Ph.D. degree in computer science from the University of Science and Technology of China, Hefei, China, and the City University of Hong Kong, Hong Kong, in 2011.

She is currently an Associate Professor with the College of Information Engineering, Nanjing University of Finance and Economics, Nanjing, China. Her research interests include networked control systems, communication protocols, software defined networking, and state estimation algorithms.

Feiyu Song received the B.S. and M.S. degrees in computer science from the Nanjing University of Finance and Economics, Nanjing, China, in 2020 and 2023, respectively.

Her research interests include complex networks and networked control systems.

Jinliang Liu received the Ph.D. degree in automatic control from Donghua University, Shanghai, China, in 2011.

He was a Postdoctoral Research Associate with the School of Automation, Southeast University, Nanjing, China, from December 2013 to June 2016. He was a Visiting Researcher/Scholar with the Department of Mechanical Engineering, University of Hong Kong, Hong Kong, from October 2016 to October 2017. He was a Visiting Scholar with the Department of Electrical Engineering, Yeungnam University, Gyeongsan, South Korea, from November 2017 to January 2018. From June 2011 to May 2023, he was an Associate Professor and then a Professor with the Nanjing University of Finance and Economics, Nanjing. In June 2023, he was with the Nanjing University of Information Science and Technology, Nanjing, where he is currently a Professor with the School of Computer Science. His research interests include networked control systems, complex dynamical networks, and time delay systems.

Xiangpeng Xie (Senior Member, IEEE) received the B.S. and Ph.D. degrees in engineering from Northeastern University, Shenyang, China, in 2004 and 2010, respectively.

He is currently a Professor with the Institute of Advanced Technology, Nanjing University of Posts and Telecommunications, Nanjing, China. His research interests include fuzzy modeling and control synthesis, state estimations, optimization in process industries, and intelligent optimization algorithms.

Prof. Xie serves as an Associate Editor for the *International Journal of Fuzzy Systems* and *International Journal of Control, Automation, and Systems*.

Engang Tian received the B.S. degree in mathematics from Shandong Normal University, Jinan, China, in 2002, the M.Sc. degree in operations research and cybernetics from Nanjing Normal University, Nanjing, China, in 2005, and the Ph.D. degree in control theory and control engineering from Donghua University, Shanghai, China, in 2008.

He is currently a Professor with the School of Optical-Electrical and Computer Engineering, University of Shanghai for Science and Technology, Shanghai. His research interests include networked control systems, cyber attack, as well as nonlinear stochastic control and filtering.

Shumin Fei received the Ph.D. degree in nonlinear systems from the Beijing University of Aeronautics and Astronautics, Beijing, China, in 1995.

From 1995 to 1997, he was a Postdoctoral Researcher with the Research Institute of Automation, Southeast University, Nanjing, China, where he is currently a Professor. His research interests include nonlinear systems, time delay system, and complex systems.